

Designing Watersheds for Integrated Development (DWID): A stochastic dynamic optimization approach for understanding expected land use changes to meet potential water quality regulations



Yu-Kai Huang^{a,*}, Ranjit Bawa^a, Jeffrey Mullen^b, Nahal Hoghooghi^c, Latif Kalin^d, Puneet Dwivedi^a

^a Warnell School of Forestry and Natural Resources, University of Georgia, USA

^b Department of Agricultural & Applied Economics, University of Georgia, USA

^c College of Engineering, University of Illinois, Urbana-Champaign, USA

^d School of Forestry and Wildlife Sciences, Auburn University, USA

ARTICLE INFO

Handling Editor - Dr. B.E. Clothier

Keywords:

Water quality
Land uses
Forestry
Stochastic dynamic optimization
Chance constraint

ABSTRACT

This study investigates the tradeoff between agricultural economic losses and potential water quality regulations at the watershed level over time. Specifically, we applied a stochastic dynamic mathematical programming approach to evaluate the impact of land use changes on agricultural economic losses under uncertain water quality regulations and crop yields. We selected the Little River Experimental Watershed in South Georgia as a case study. Seven potential water pollution reduction trajectories for total phosphorus (TP) were developed. The proposed model applied a chance-constraint technique to allow some degree of uncertainty in meeting the water quality standards. The result shows that agricultural profits decrease when uncertainties are considered at the watershed level. The findings further show that uncertainties of meeting the water quality standard expedited the land use transition from croplands to forestlands and magnified the share of forestlands, highlighting the crucial role of forests in managing water pollution in the selected watershed. The results also indicate that under a moderate pollution reduction scenario, an economic loss of \$232/ha/yr is expected to achieve a 16 % reduction in TP concentration. In a more ambitious pollution mitigation scenario, agricultural economic losses are expected to be \$778/ha/yr and may result in a 45 % decrease in TP concentration. The modeling approach developed in Designing Watersheds for Integrated Development (DWID) could easily feed into those policy deliberations which operate at the interface of economics and water-related policies for ensuring sustainable management of watersheds worldwide.

1. Introduction

Agricultural runoff is the primary source of water quality issues in the United States, resulting in a situation where about 58 % and 34 % of rivers and streams in the United States are rated as “poor” due to high phosphorus and nitrogen concentrations, respectively (USEPA, 2020). Considering the role of existing agricultural lands in water pollution, the United States Environmental Protection Agency (USEPA) spends about 40 % of Clean Water Act grants to control nonpoint source pollution from working farms and ranches (USEPA, 2014). On the contrary, forestlands have been typically identified as crucial in improving water quality in the United States. For example, forested watersheds have

consistently been shown to have lower nutrient yields with better aquatic biological conditions than non-forested watersheds across the Southern United States (West, 2002). Although silvicultural activities may have some negative impacts on water quality due to changes in hydrological responses of watersheds, reductions in dissolved oxygen content, increases in the nutrient content of streams, and effects on aquatic habitat and forested wetlands, these effects are mostly context-specific (Neary et al., 2009). These adverse effects can also be controlled to a larger extent by implementing best management practices (BMPs) and following other sustainability standards (Jackson, 2012). In the United States, the implementation rate of silviculture BMPs is already at 91 % and still increasing (Cristan et al., 2018).

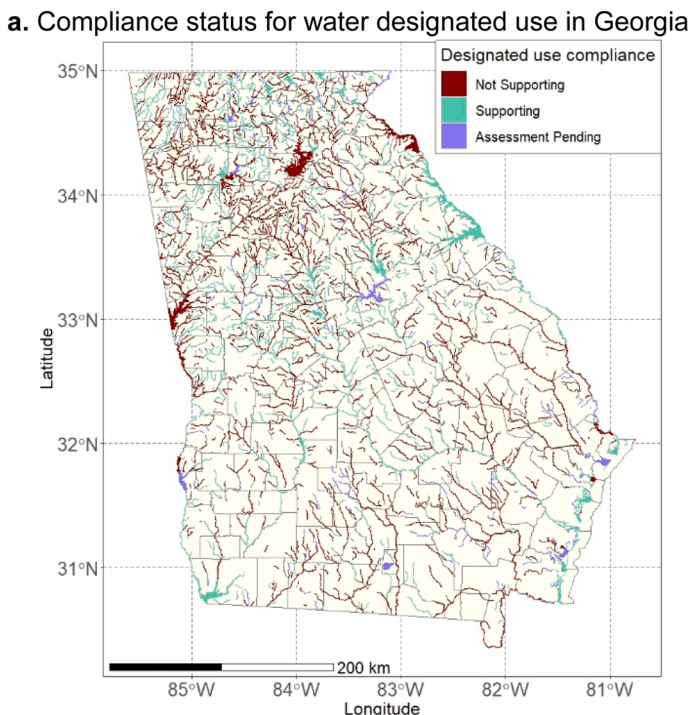
* Correspondence to: Warnell School of Forestry and Natural Resources, University of Georgia, 180 E Green St, Athens, GA 30602, USA.
E-mail address: yh53616@uga.edu (Y.-K. Huang).

Georgia, a state in the Southern United States, is facing significant challenges in maintaining water quality. The [Georgia Environmental Protection Division \(2020\)](#) indicates that 57.7 % and 40.8 % of surveyed stream/river and lakes/reservoirs, respectively, did not meet the limits set for their designated uses between 2018 and 2019. Fig. 1a shows the spatial distribution of water bodies in Georgia that do not meet their designated uses. According to the [Georgia Environmental Protection Division \(2020\)](#), pollution from nonpoint sources is primarily responsible for water quality issues in Georgia (Fig. 1b). Almost 94 % and 65 % of water quality issues in rivers/streams and lakes/reservoirs were attributed to nonpoint pollution sources in Georgia, respectively ([Environmental Protection Division, 2020](#)). Among various nonpoint pollution sources, agriculture is a crucial source affecting Georgia's water quality. This is especially true as farmers planted 1.3 million hectares of land in 2020 under various summer crops (e.g., cotton, peanut, soybean, etc.) and perennial crops (e.g., hay, pecan) across the state, covering 8.6 % of the total land in the state ([USDA-NASS, 2019](#)).

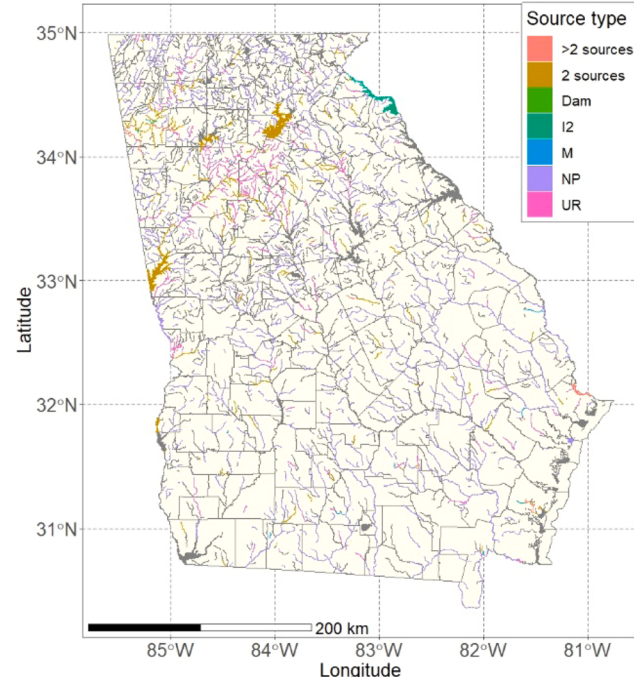
Improving water quality is vital to safeguard Georgia's economy over time. Afforestation could be an effective way to ensure improvements in water quality. Several studies have analyzed the impact of afforestation on improving water quality across the Southern United States. [Tu \(2011a\)](#) applied geographically weighted regression to investigate the spatial relationship between land use and water quality and found that the percentage of forests is an indicator of good water quality. [Gunter et al. \(2005\)](#) studied the effect of demographic and spatial factors on the probability of adopting land use regulations to improve water quality in Georgia, Florida, and Louisiana using a logistic regression model and indicated reliance on forestry/agriculture as a key component to determine the tendency of adopting local regulations. In addition to the above regression-based studies, several studies have used various modeling approaches to assess the impact of land use change on water quality across the United States ([Bhattarai et al., 2008; Isik et al., 2013; Pennington et al., 2017; Rabotyagov et al., 2010; Singh et al., 2015](#)).

Similarly, several studies have used other modeling approaches to assess the impact of environmental regulations on water use ([Boadu et al., 2007; Chen et al., 2006; Gillig et al., 2001](#)) and water quality ([Gaddis et al., 2014](#)) relative to land use changes.

Even though there is a relatively large body of existing literature regarding modeling the effect of land use change on water quality, these studies are limited for several reasons. First, existing regression-based studies are limited to providing insights into optimal rotation decisions and associated whole stem volumes over time. Second, existing forest modeling literature, especially in the Southern United States, is short on assessing the effect of economic and policy factors on water quality and forest management derived from longer-term economic optimization models. Third, very few studies ([Kaim et al., 2020; Sunandar et al., 2014; Whittaker, 2005](#)) have considered hydrological and economic factors together to better capture the effect of physical land use changes on water quality and economy. Finally, there is little discussion about how the uncertainty of meeting a water quality regulation affects land use changes. It is crucial to assess the economic and environmental tradeoffs relative to possible water quality regulations in light of changing land use at a watershed level over space and time. Therefore, we extended the original modeling framework of Designing Watersheds for Integrated Development (DWID), an integrated hydrological-economic optimization-based algorithm from [Bawa \(2021\)](#), by incorporating chance constraints to capture the uncertainty of nutrient discharge at the watershed outlet. Specifically, we first used the Soil and Water Assessment Tool (SWAT) to generate hydrological data. We then developed a stochastic mathematical programming model for ascertaining the tradeoffs between profits and environmental regulations in light of changing land use spatially and temporally. Using data from the SWAT model can provide helpful information regarding hydrology, crop growth, nutrients, and sediment loads at the watershed level while simulating land use changes. Our study fills these critical gaps and advances the literature for improving water quality in Georgia



a. Compliance status for water designated use in Georgia



b. Pollution sources for water bodies in Georgia

Fig. 1. Distribution of water bodies in Georgia that did not meet water quality standards for designated usages under Section 305(b)/303(d) of the Clean Water Act and their causes. In Panel a., 'Supporting' indicates a water body that meets standards by supporting the designated use; 'Not Supporting' indicates a water body that does not meet the designated use standards. In Panel b., I2 denotes industrial site runoff; M denotes municipal point source discharge; NP denotes nonpoint source; UR denotes urban runoff.

Source: [Environmental Protection Division \(2020\)](#).

and beyond.

2. Methods and materials

2.1. Study area

2.1.1. Little River Experimental Watershed (LREW)

The study area is the Little River Experimental Watershed (LREW) in the headwaters area of the Suwannee River Basin, located in the recharge area of the Upper Floridan Aquifer, which is one of the most productive aquifers in the world (USGS, 2016). The LREW is 334 km² and overlays Turner County, Tift County, and Worth County in Georgia, United States (Fig. 2). The population in this region is growing, and associated economic activities are expanding, although agriculture and silviculture are the primary land uses. There are 198 sub-basins at the HUC-12 watershed level (USGS, 2022) in this study, and the period of analysis spans from 1997 to 2005, limited by the availability of experimental data in LREW. The LREW primarily consists of low gradient streams with channel slopes ranging from 0.1 % to 0.4 % (Bosch and Sheridan, 2007). According to Bosch et al. (2020), the row crop area has increased from 31 % to 36 % between 1975 and 2014 in the study region, but its maximum share reached 51 % in 1985. On the other hand, forest cover decreased from 49 % to 43 % in the same period.

In summary, the LREW is an agricultural-dominated area with a significant portion of forestlands. Based on the dominant categories identified by the National Land Cover Database NLCD, (2004) (Fig. 2) and the relevance of the study, the type of land use considered in this study includes Bermuda hay, corn, cotton, peanut, and forest (classified as hardwood and softwood). Note that woody wetlands act more like riparian buffers, so they are not considered part of the actively managed forestlands and are not included in our analysis. Land use classes considered in this study are for individual crops and were selected based on the United States Department of Agriculture, National Agricultural Statistics Service (USDA-NASS) datasets for agricultural land use in the SWAT model (for more details, refer to Section 3).

2.1.2. Water quality regulation

Excess nutrients in a water body can deteriorate water quality by fostering algae blooms, accelerating plant growth, and lowering dissolved oxygen from decomposition (USEPA, 2015). According to the USEPA (2014), an acceptable range of total phosphorus (TP) for

aggregate ecoregions for rivers and streams is 0.01 mg/L to 0.08 mg/L. Nevertheless, the average TP concentration in the study area was 0.46 mg/L from 1974 to 2014 (Bosch et al., 2020), which is higher than the USEPA's standard. Among different land use, agricultural lands produce more TP than other land surfaces (Duffy et al., 2020; Yong and Chen, 2002). Thus, this study aims to develop a dynamic stochastic mathematical programming approach for exploring possible water pollution reduction trajectories to mitigate TP concentration among different land use while limiting potential landowners' losses induced by compliance with water quality regulations. The incorporation of stochasticity has significantly expanded the capability of the original DWID modeling framework.

2.2. SWAT model

2.2.1. Overview

SWAT is a process-based and semi-distributed model that can simulate hydrology, crop growth, nutrients, and sediment loads (Arnold et al., 2012). SWAT is one of the most broadly applied large-scale watershed simulation models in Total Maximum Daily Load (TMDL) analyses and water resource planning. Its applications have included predicting the impact of land management practices on nutrient yields from agricultural land use in large complex watersheds with varying soils, land use, and management conditions over long periods (Gassman et al., 2007; Shrestha et al., 2019).

We used ArcSWAT 2012 interface to set up the model using the 30 m Digital Elevation Model (DEM) (USDA-NRCS, 2021), Soil Survey Spatial Tabular (SSURGO 2.2) soils data, and National Land Cover Dataset (NLCD, 2004). Daily precipitation and min/max temperature data were obtained from Parameter-elevation Regressions on Independent Slopes Model (PRISM) for the SWAT model (Table 1). We followed Van Liew

Table 1
Data feed used to produce SWAT simulations.

Parameter	Source
Elevation (30 m)	USDA-NRCS (2021)
Soil series	Soil Survey Geographic Database (SSURGO V2)
Land cover type	NLCD (2004)
Precipitation	Precipitation Regression on Independent Slopes Model (PRISM)
Temperature	Precipitation Regression on Independent Slopes Model (PRISM)

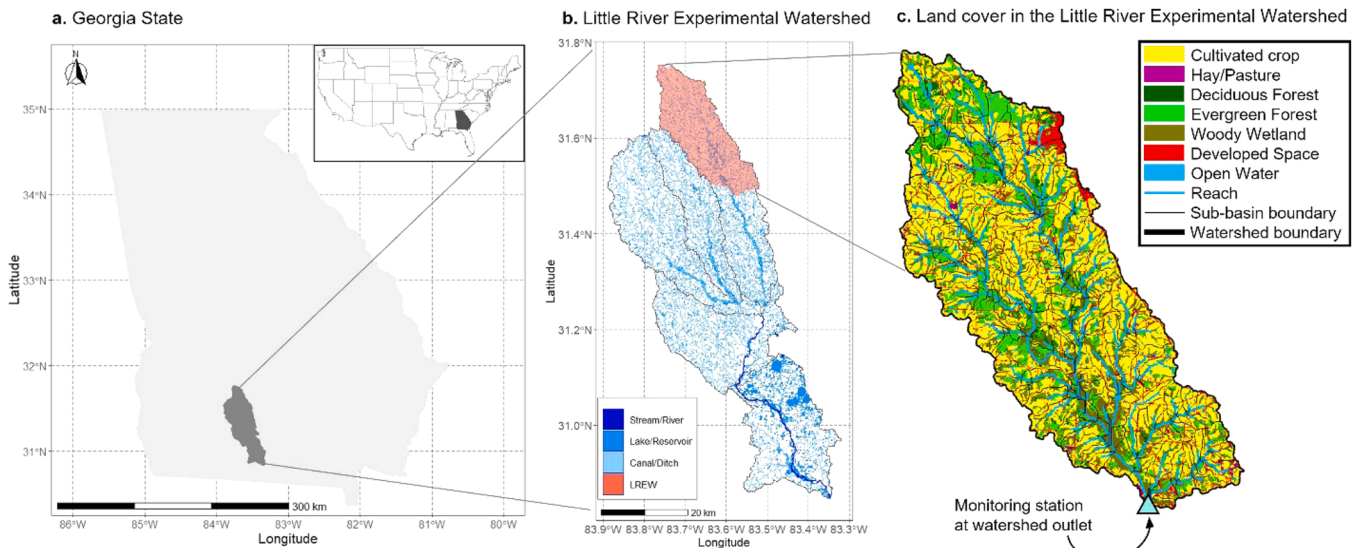


Fig. 2. Study area. The figure illustrates the location of the Little River Experimental Watershed (LREW) within the Litter River Hydrologic unit (HUC-10), Georgia, United States.

Maps were produced using data from USGS, (2022) (Panels a and b) and land cover data from NLCD (2004) (Panel c).

et al. (2005) and chose the Hargreaves method (Hargreaves et al., 1985) for estimating potential evapotranspiration (PET). Using topographic information, the SWAT model divided the watershed into 198 sub-basins. Subsequently, each sub-basin was divided into hydrologic response units (HRUs) with unique combinations of land use, soil, and slope (Arnold and Fohrer, 2005). Three slope classes were used for HRU classification: 0–5 %, 5–10 %, and above 10 %. The threshold of 20 %, 10 %, and 5 % for soil, land use, and the slope was applied to reduce the number of HRUs (total 1272 across 198 sub-basins). We obtained an estimate of management operations (planting dates, fertilizer application rate and type, crops yield, and harvesting dates) for the LREW from an extension agronomist at the University of Georgia and USDA-NASS (1997). The SWAT setup and crop category were determined by land cover data from NLCD 2006 and Cropland Data Layer (CDL) data from USDA-NASS. A 3-year peanut-corn-cotton rotation was applied in the model for all the peanut, corn, and cotton fields. Amounts of 134 and 65 kg N/ha in the form of elemental nitrogen fertilizer were applied in corn and cotton fields, respectively. The amount of 50 kg P/ha of phosphorus fertilizer (as P_2O_5) was applied in both corn and cotton fields. For hay land use, urea (200 kg/ha) with two applications in May and June, and elemental P (60 kg/ha) were applied. We used the ‘harvest only’ operation in SWAT that occurred twice a year. A baseflow separation technique (Arnold et al., 1995) was used to initialize the value of the baseflow recession constant (ALPHA_BF). We made relative adjustments to ALPHA_BF during the model calibration.

2.2.2. Calibration & validation

The Sequential Uncertainty Fitting algorithm (SUFI-version 2) in the SWAT Calibration and Uncertainty Programs platform (Abbaspour et al., 2015; Abbaspour et al., 2007) was used to calibrate and validate the model for streamflow, TP, and sediment at daily time step at the outlet of LREW. The SUFI-2 combines optimization with uncertainty analysis. Uncertainties in the parameters result in model output uncertainties, quantified as the 95 % prediction uncertainty (95PPU) band between the 2.5 % and 97.5 % levels of the cumulative distribution of an output variable using Latin hypercube sampling (Abbaspour et al., 2007). The model was calibrated for the entire LREW.

The observed data from the USDA-ARS gauging station at the main watershed outlet between 1997 and 2005 were used with a four-year model initialization (1993–1996) followed by a five-year calibration (1997–2001) and four years model validation (2002–2005). To evaluate the model performance, we used two quantitative error statistics: Kling-Gupta efficiency (KGE) (Gupta et al., 2009) and the Percent Bias (PBIAS). The KGE contains three components: correlation (r), present bias (μ_s/μ_o), and variability ratio (σ_s/σ_o) between the simulated (s) and observed (o) variable; μ and σ are the mean and standard deviation of the variable, respectively:

$$KGE = 1 - \sqrt{\left\{ (r-1)^2 + \left(\frac{\mu_s}{\mu_o} - 1 \right)^2 + \left(\frac{\sigma_s}{\sigma_o} - 1 \right)^2 \right\}} \quad (1)$$

KGE ranges from $-\infty$ to 1, with a value closer to 1 representing a relatively accurate model. KGE overcomes the disadvantage of Nash-Sutcliffe efficiency (Nash and Sutcliffe 1970) in underestimating peak flow prediction (Gupta et al., 2009). PBIAS measures the average tendency of the predicted data to be larger or smaller than observed values. It also measures over- and underestimation of bias (Moriasi et al., 2007):

$$PBIAS = \frac{\sum_{i=1}^n (o_i - s)}{\sum_{i=1}^n o_i} \times 100 \quad (2)$$

The optimum value for PBIAS is 0 %, where values close to zero indicate better model prediction. Model overestimation is signified by $PBIAS < 0$ % and underestimation happens when $PBIAS > 0$ % (Moriasi et al., 2015).

In addition to these parameters, we incorporate biophysical

parameters for major crops in the LREW in our calibration process. Parameters controlling nutrients and sediment loads were selected based on the literature (Abbaspour et al., 2007; Moriasi et al., 2012). Parameters controlling streamflow and plant growth were calibrated first, followed by sediment and phosphorus.

We used average annual USDA-NASS crop yield observed data (except for forest classes). After the streamflow was calibrated, crop parameters were adjusted to simulate crop yields (Table 2). Forest growth was not calibrated in the model. Instead, the forest parameters were borrowed from Haas et al. (2022), where they addressed loblolly pine (*Pinus taeda L.*) and slash pine (*Pinus elliotti*), but the methodology applies to most forest species and can be applied widely in the southeastern region of the United States. We then used observed NASS data to simulate the crop yields in the study area. The 2002–2003 period (2 years) was used for TP and sediment loads.

2.2.3. Nutrient load assignment

2.2.3.1. Contribution modeling. SWAT routes flow and nutrient loadings using a routing scheme based on the channel network that connects the outlets of sub-basins to the watershed’s primary outlet. As one would expect, the sum of nutrient loadings leaving each sub-basin will not be equal to the nutrient load at the watershed outlet due to the instream biochemical reactions. To account for TP loss and transformations at each sub-basin, we used an approach that assesses TP load contributions from each sub-basin over simulation periods at the watershed outlet (see Kalin and Hantush, 2009; Noori et al., 2016; Saghafian and Khosroshahi, 2005) and as shown in Fig. 5. Therefore, after calibrating and validating the SWAT model, we defined a virtual rain gauge for each sub-basin in the watershed. The rain gauges were switched off in successive series to find the contribution of each sub-basin to the nutrient loads at the watershed outlet (see Fig. 5). The software R V.4.0.2 with extension package SWATplusR (Schuerz, 2019) was employed as a part of this analysis by interacting with our SWAT project to help execute efficient simulation runs across all sub-basins (for TP).

2.2.3.2. Land use assumptions. Adjusted TP loadings calculated at the sub-basin level were further broken down by land use. The model framework considers six land uses: Bermuda hay, corn, cotton, peanut, and forest, classified as softwood and hardwood. The default SWAT setup was used for forest management, which assumes no fertilizer use, no thinning, and a maturity of 10 and 30 years for deciduous and

Table 2

The selected crop parameters for cotton, corn, peanut, and Bermudagrass in the SWAT model and their initial range, default and fitted values.

Crop Parameter	Parameter description	Initial range	Default value	Fitted value
BIO_E	Radiation use efficiency or biomass energy ratio (kg/ha)/(MJ/m ²)	10–90	Cotton: 15 Corn: 39 Peanut: 20 Bermudagrass: 35	Cotton: 18 Corn: 36 Peanut: 27 Bermudagrass: 35
	Maximum potential leaf area index (m ² /m ²)		Cotton: 4 Corn: 6 Peanut: 4 Bermudagrass: 4	Cotton: 5 Corn: 5 Peanut: 4 Bermudagrass: 4
	Fraction of growing season when growth declines		Cotton: 0.95 Corn: 0.7 Peanut: 0.75 Bermudagrass: 0.99	Cotton: 1.1 Corn: 1 Peanut: 1 Bermudagrass: 1.2
	Harvest index for optimal growing season (kg/ha)/(kg/ha)		Cotton: 0.4 Corn: 0.5 Peanut: 0.4 Bermudagrass: 0.9	Cotton: 0.4 Corn: 0.5 Peanut: 0.4 Bermudagrass: 0.9

evergreen forests, respectively. An additional land use category, extra, which is meant to capture barren land, is also included. The crop type in our analysis is therefore composed of a total of seven classes. TP loadings for each crop in each sub-basin were calculated as the weighted average of loadings, weighted by SWAT reported crop yields at the HRU level. As an initial step, daily TP loadings, corresponding to each HRU by crop type for each year were obtained from calibrated SWAT output. Values were summed over days to arrive at annual values corresponding to each HRU. Computing the average across all years and HRU for each crop then served as the basis for constructing relative weights among crop type. The created crop coefficients were subsequently multiplied by the adjusted nutrient load recorded at each sub-basin i to derive specific nutrient allocation by crop type. Land classified as Extra was assumed to produce zero nutrient loadings. (Fig. 3).

2.3. Economic model

2.3.1. Selected scenarios

This study integrates total phosphorus (TP) data from a SWAT model and uses the midpoint of the USEPA criteria, 0.045 mg/L, as a water quality regulation goal. Then seven possible water pollution reduction scenarios were established to depict potential water quality improvement paths from the concentration (0.57 mg/L) to the USEPA standard (0.045 mg/L). The scenarios of phosphorus concentration limits over the study period are described in Table 3, and the corresponding water quality improvement paths are illustrated in Fig. 4.

2.3.2. Modeling land use decisions

The stochastic dynamic optimization model developed here is used to investigate landowners' responses to different water quality regulation scenarios over time. The model assumes landowners to be risk-neutral and to maximize the present value of a stream of expected future returns to the land (Z) as shown in Eq. (3):

$$\text{Max } Z = \sum_j \sum_i P_{j,t} Y_{j,i,t} H_{j,i,t} - \sum_j \sum_i I_{j,t} H_{j,i,t} - \sum_j \sum_i C_{j,i,t,r} X_{j,i,t,r} \quad (3)$$

where the decision variables in this model are $H_{j,i,t}$ and $X_{j,i,t,r}$. The former is hectares harvested for cropland j in sub-basin i at the beginning of year t , and the latter is hectares converted from cropland j to cropland r in sub-basin i at the end of year t . Note that subscripts j and r have the same dimension length of six, indicating Bermuda hay, corn, cotton, peanut, hardwood, and softwood, respectively. The decision variables are associated with the following price parameters: $P_{j,t}$ is a set of discounted annual real crop prices (in US\$/kg), expressed in 1997 dollars, for crop j in year t ; $Y_{j,i,t}$ is an annual crop yield (in kg/ha) for crop j in sub-basin i in year t produced from the SWAT model; $I_{j,t}$ is a discounted crop production cost (in US\$/ha) for cropland j in year t ; and $C_{j,i,t,r}$ is a discounted cost (in US\$/ha) of changing land use from cropland j to cropland r in sub-basin i in year t . The above price terms were all discounted at 4.2 %, which is based on a range of 3–7 % commonly applied in the social discounting of environmental investments (Li and Pizer, 2021; Office of

Table 3
Scenario descriptions for phosphorus concentration limits.

Scenario	Description
S0	No regulation.
S1	Start to reduce the TP concentration limit in the 5th year and linearly decrease to the USEPA standard.
S2	Start to reduce the TP concentration limit in the 3rd year and linearly decrease to the USEPA standard.
S3	Start to reduce the TP concentration limit in the 1st year and linearly decrease to the USEPA standard.
S4	Linearly decrease the TP concentration limit to the USEPA standard within 7 years.
S5	Linearly decrease the TP concentration limit to the USEPA standard within 5 years.
S6	Linearly decrease the TP concentration limit to the USEPA standard within 3 years.

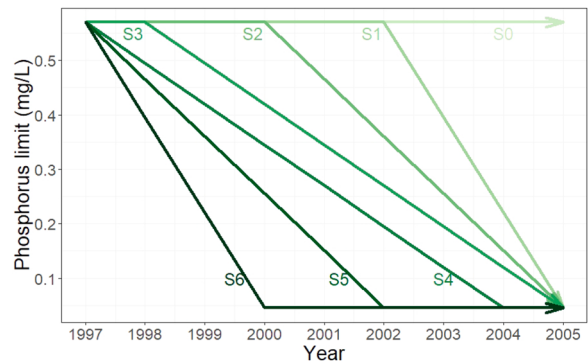


Fig. 4. Water quality improvement path scenarios. This figure depicts the scenarios for the phosphorus concentration limit ($\delta_{t,s}$) in Eqs. (8 to 10). The phosphorus concentration is 0.57 mg/L in the baseline scenario (S0), which is 0.57 mg/L produced from the SWAT model and calculated over all cropland types across 198 sub-basins during the study period. The midpoint of the USEPA standard is 0.045 mg/L. The above policy scenarios demonstrate possible paths to reduce the phosphorus concentration from 0.57 mg/L to 0.045 mg/L.

Management and Budget, 1992).

Landowners maximize profits formulated in Eq. (3) subject to the following constraints. Eq. (4) ensures the total allocated land for all crops ($L_{i,t}$) does not exceed the total available land ($A_{i,t}$) in each sub-basin and year:

$$\sum_j L_{j,i,t} \leq A_{i,t}, \forall i, t \quad (4)$$

In each sub-basin and year, harvested cropland ($H_{j,i,t}$) must not exceed the total allocated land ($L_{j,i,t}$) for each crop, as expressed in Eq. (5):

$$H_{j,i,t} \leq L_{j,i,t}, \forall j, i, t \quad (5)$$

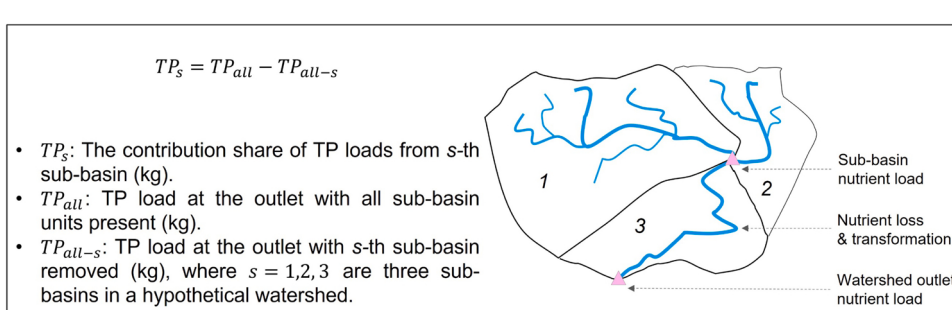


Fig. 3. Schematic of TP load contribution from each sub-basin over simulation periods for a hypothetical watershed with 3 sub-basins (there are 198 sub-basins in this study).

Eq. (6) imposes a constraint in which hectares converted from cropland j to cropland r ($X_{j,i,t,r}$) must not exceed hectares harvested for each crop ($H_{j,i,t}$) in each sub-basin and year. The land conversion is assumed to occur at the end of a given year t after harvest.

$$\sum_r X_{j,i,t,r} \leq H_{j,i,t}, \forall j, i, t \quad (6)$$

To ensure the total allocated land satisfies the land use balance in each sub-basin and year, **Eq. (7)** requires allocated cropland in a current year ($L_{j,i,t}$) is equal to hectares harvested for crop j in the previous year ($H_{j,i,t-1}$) plus the net hectares converted from other crops to crop j in the previous year.

$$\sum_j L_{j,i,t} = \sum_j H_{j,i,t-1} + \sum_{r=j} X_{j,i,t-1,r} - \sum_{r=j} X_{j,i,t-1,r}, \forall i, t \quad (7)$$

Finally, landowners' land use decisions are restricted by the hypothetical water quality regulation constraint based on the water pollution criteria of the policy scenario being evaluated:

$$\sum_j \sum_i \mu_{j,i} H_{j,i,t} \leq \delta_{t,s}, \forall t, s \quad (8)$$

where $\mu_{j,i}$ is mean of phosphorus concentration per hectare for crop j in sub-basin i . $\delta_{t,s}$ is the phosphorus concentration limit (in mg/liter) in year t under criteria scenario s illustrated in Fig. 4 and Table 3.

Eq. (8) assumes that there is no probability specified for landowners to meet the required phosphorus concentration limit in each time step. Hereafter, the model in **Eq. (8)** is referred to as the "deterministic model." The assumption that water quality targets will be met randomly, however, may be less informative. Hence, following the related literature (Ellis, 1987; Jacobs et al., 1997; Wang et al., 2015), a stochastic chance constraint for achieving the water quality criteria is developed using **Eq. (9)**:

$$\Pr \left[\sum_j \sum_i \mu_{j,i} H_{j,i,t} \leq \delta_{t,s} \right] \geq \alpha, \quad \forall t, s \quad (9)$$

Eq. (9) ensures the likelihood of meeting the required phosphorus concentration in year t is realized at a minimum probability α , reflecting a more informative aspect of probabilistic violations of water quality standards. The α values used in this study are 90 %, 95 %, and 99 %. Following chance-constraint water management references (Cardwell and Ellis, 1993; Ellis, 1987; Fujiwara et al., 1986; Sethi et al., 2006; Wang et al., 2015; Zhou et al., 2018), **Eq. (9)** can be further converted into the following formula:

$$\sum_j \sum_i \mu_{j,i} H_{j,i,t} + \sum_i \Phi^{-1}(\alpha) \cdot \sqrt{\sum_j \sum_i (\sigma_{j,i} H_{j,i,t})^2} \leq \delta_{t,s} \quad (10)$$

where $\sigma_{j,i}$ is variance of phosphorus concentration per hectare for crop j in sub-basin i . $\Phi^{-1}(\bullet)$ is the cumulative distribution function of a standard normal random variable, and $\Phi^{-1}(\bullet)$ is the inverse function. A detailed derivation of **Eq. (10)** from **Eq. (9)** can refer to Jacobs et al. (1997), and mathematical notation descriptions for the entire model are summarized in Table 4. **Eq. (10)** is hereafter referred to as the "stochastic model." Note that when α is 50 %, the stochastic model will turn to the deterministic one with the average phosphorus concentration.

2.3.3. Crop yield simulation

To investigate how profits change under uncertain crop yields, a simulation technique is used to develop stochastic crop yields. The simulation procedure is described as follows:

Step 1: Calculate annual mean and variance for crop j in sub-basin i ($\mu_{j,i}$ and $\sigma_{j,i}$).

Step 2: Use $\mu_{j,i}$ and $\sigma_{j,i}$ to construct a normal distribution for each crop type in each sub-basin $Normal_{j,i}(\mu_{j,i}, \sigma_{j,i}^2)$.

Table 4
Mathematical description of the optimization model.

Subscripts	
j	Original cropland type harvested at the beginning of a year
r	New cropland type converted at the end of a year
i	Sub-basin
t	Year
s	Regulation scenario
Decision variables	
$H_{j,it}$ (hectares)	Harvest for cropland j in sub-basin i at the beginning of year t
$X_{j,it}$ (hectares)	Convert cropland j to cropland r in sub-basin i at the end of year t
Variables	
Z (US\$)	Aggregated landowner profits
$P_{j,t}$ (US\$/kg)	Discounted annual crop price for crop j in year t
$Y_{j,it}$ (kg/hectare)	Annual crop yield for crop j in sub-basin i in year t
$I_{j,t}$ (US \$/hectare)	Discounted crop production cost for cropland j in year t
$C_{j,it}$ (US \$/hectare)	Discounted cost of changing land use from cropland j to cropland r in Sub-basin i in year t
$L_{j,it}$ (hectares)	Allocated annual cropland j in sub-basin i in year t
A_{it} (hectares)	Total available land in sub-basin i in year t
$\mu_{j,i}$ (mg/liter)	Mean phosphorus concentration for cropland j in year t
δ_{ts} (mg/liter)	Phosphorus concentration criteria s in year t

Step 3: Draw a crop yield value from each normal distribution constructed from Step 2.

Step 4: Input the drawn yield values from Step 3 into the objective function (i.e., **Eq. 3**), solve the optimization problem and record the resulting outcome.

Step 5: Repeat Step 2 to Step 4 for 500 times and calculate the simulated mean and standard deviation. Note that simulation for stochastic models produced some infeasible results, which were excluded when calculating the simulated mean and standard deviation.

For the simulation results, 170 out of 3,500 (= 7 scenarios \times 500) simulation repetitions were infeasible and/or non-optimal solutions, which were excluded when calculating the simulated mean and standard deviation. We summarized all uncertainty sources considered in this study as a 2 by 2 matrix, as shown in Table 5.

2.3.4. Data for parameters in the economic model

There are two sets of parameters used in the stochastic dynamic optimization model: economic and hydrological. The economic parameters include annual crop prices (in US\$/kg), annual crop production costs (in US\$/ha), and land use conversion costs (in US\$/ha). The annual crop price data for corn, cotton, Bermuda hay, and peanut were retrieved from USDA-NASS (2019). Prices for hardwood and softwood were from TMS (2019) and were annualized over 25 years. Crop production costs for annual crops used historical expected cost budgets for the study area from the University of Georgia (2020). Forest crop costs were calculated as the sum of average annual costs over a 25-years rotation, including fertilizers, herbicides, machine planting, mechanical site preparation, and prescribed burning (Maggard and Barlow, 2016). Land use conversion cost estimates were obtained from the University of Georgia (2020). The costs of switching forest to agricultural lands are at least \$4942/ha and \$6177/ha for softwood (pine) and hardwoods, respectively. Based on consultation with field experts, the above costs include

Table 5
Summary of the uncertainty sources, modeling approaches, and associated results.

	Crop yield uncertainty (Modeled by resampling simulation)			
	N	Y	SP50-DY	SP50-SY
Water quality uncertainty (Modeled by the chance-constrained formula)	N	Y	SP50-DY	SP50-SY
	Y		SP-DY	SP-SY

Note: SP represents stochastic phosphorus concentration. Similarly, DY represents deterministic yields while SY represents stochastic yields.

costs for excavator services to pull and pile stumps and clear the land of stumps. Conversion costs from Bermuda hay to other agricultural croplands were estimated at \$179.12/ha, considering incurred costs for prepping lands with necessary fertilizer and herbicide application.

The hydrological parameters were from the SWAT model. They were produced by the SWAT model, consisting of crop yields, surface runoff, and phosphorus load. The SWAT model was initially calibrated over five years (1997–2001) and validated over four years (2002–2005) at the outlet. The model considers seven land use types: Bermuda hay, corn, cotton, peanut, forest (classified as hardwood and softwood), and barren land. Barren lands were assumed to produce zero TP loadings. A summary of data sources is presented in Table 6.

3. Results

3.1. SWAT modeling results

3.1.1. SWAT calibration and validation

The calibration process for the LREW started with 36 hydrologic and biophysical parameters. After 1000 simulations, the most sensitive flow and biophysical parameters were identified, and these are listed in Table 7 in order of decreasing sensitivity. The most sensitive parameters were effective hydraulic conductivity of the alluvium in the main channel (CH_K2.rte), groundwater delay time (GW_DELAY.gw), the fraction of growing season when leaf area begins to decline (DLAI.plant.dat), runoff curve number 2 (CN2.mgt), and available water capacity of the soil layer (SOL_AWC.sol). Parameter values should be considered after calibration to avoid unrealistic simulations. For instance, the fitted values for SOL_AWC in the SWAT model for crops and forest soil ranged from 0.06 to 0.07, which was comparable to the measured weighted average SOL_AWC of 0.057 for the Tifton soil series by Hubbard (1985). CN2 for the main crops and forest (evergreen and deciduous) were reduced by 12 %, resulting in a better adjustment to streamflow predictions. The model fit was deemed satisfactory for streamflow calibration and validation with a daily KGE of 0.80 and 0.71 and PBIAS of -2.5 and 3.8, respectively. The observed streamflow, TP, sediment loads, the model best fit, and the 95 PPU band for calibration and validation periods are shown in Fig. 5. After the model was calibrated for hydrology and biophysical parameters, the narrow ranges for selected parameter values were fixed, and the model was calibrated for sediment load at the watershed outlet using 14 parameters. The SWAT model for TP, sediment loads, and streamflow are shown in Table 8 for the calibration and validation periods. (Fig. 5).

The most sensitive parameters for sediment load were the exponent parameter for calculating sediment re-entrained in channel sediment routing (SPEXP.bsn), a linear parameter for calculating the maximum amount of sediment that can be re-entrained during channel sediment routing (SPCON.bsn), and the cover factor for the effect of land cover on erosion (USLE_C.plant). The SPEXP and SPCON are parameters used to calculate the maximum amount of sediment that can be transported

from a reach. The fitted value for SPEXP and SPCON in our model was 1.210 and 0.001, respectively. The daily KGE was 0.43 and 0.57 for the calibration and validation period, respectively, with PBIAS of -2.5 % for the calibration period and 0.2 % for the validation periods (Table 8).

The most sensitive TP parameters were residue decomposition coefficient (RSDCO.bsn), phosphorus enrichment ratio for loading with sediment (ERORGP.hru), and the cover factor for the effect of land cover on erosion (USLE_C.plant) (Table 7). The fitted value for RSDCO and ERORGP was 0.07 and 2.58, respectively. The daily KGE for TP load was 0.63, with PBIAS of 0.4 % for the calibration period and KGE of 0.35 with PBIAS of 2.8 % for the validation period. The model performance for daily TP at the watershed outlet was evaluated as "satisfactory" with daily KGE > 0.35 and PBIAS $\leq \pm 30\%$. The lower KGE for the validation period was expected because the observation data for TP loads were sparse for that period (compared with daily observations for streamflow).

3.1.2. Nutrient contribution

Since this study focuses on reducing TP concentration, the SWAT model results are presented only for TP and sediment. Upon calibration and validation in SWAT, TP loading linked to a given HRU for each day for each year was summed across days to arrive at annual values before averaging across all years for each HRU. (Fig. 6) A comparison of TP loadings by crop type is presented in Fig. 7. Average annual TP loadings in Fig. 7 were the lowest for forest land cover. Softwood was associated with slightly higher loads, estimated at 0.023 kg/ha per year, compared with 0.021 kg/ha per year for hardwoods. Bermuda was reflective of the highest TP load out of the six crops at 0.396 kg/ha per year. A previous study reports that TP from pasture has the range of 0.14–4.90 kg/ha/yr, which covers our annual average TP load (Reckhow et al., 1980). Similarly, cotton shows a fairly large number of outliers in the upper range, averaging 0.252 kg/ha per year. Peanut and corn trail behind with estimated average annual loads of 0.081 and 0.072 kg/ha, respectively.

3.2. Economic modeling results

3.2.1. Summary statistics for economic variables and parameters

Fig. 8 presents an overview of the key variables/parameters, including crop yields ($Y_{j,i,t}$), revenues ($P_{j,i,t}Y_{j,i,t}$), crop production costs ($I_{j,t}$), and sub-basin level TP concentration used for calculating mean TP concentration (μ_{jt}). Fig. 8a shows that hay and woody crops have a relatively higher mean yield, and woody crops tend to have larger variability compared to other crops. Overall, cotton and peanut are the most valuable crops among the study crops, as shown in Fig. 8b. Nevertheless, corn, cotton, hay, and peanut are also relatively costly compared to woody crops.

3.2.2. Impact of water pollution reduction on profit changes

Profit estimates obtained from the deterministic and stochastic dynamic optimization models under seven water pollution reduction scenarios are presented in Fig. 9a. In the deterministic model, the total profit is estimated to be \$1340/ha/yr when the water quality standard remains constant over the study period (Scenario 0). However, it declines from \$1340/ha/yr to \$695/ha/yr (i.e., a 48 % reduction) when the water quality regulation switches from the no restriction scenario (Scenario 0) to the strictest scenario (Scenario 6).

In the case of the stochastic model, the results shown in Fig. 9a reveal the impact of the policy uncertainty on profits under three probabilistic scenarios (i.e., 90 %, 95 %, and 99 % described in Eqs. 9 and 10). These stochastic optimization results assume a 90 %, 95 %, and 99 % chance to meet the water quality standard, respectively, instead of the 50 %, assumed in the deterministic model. Overall, the stochastic model results have a similar pattern as the deterministic results but have relatively lower profit estimates. The estimated total profit with a 95 %

Table 6
Various data sources used for the economic model.

Variables	Dimensions	Source
Crop yield	6 crops, 198 sub-basins, 9 years	SWAT model
Crop price	6 crops, 9 years	USDA NASS (2019), TM (2019)
Crop cost	6 crops, 9 years	UGA extension historical crop budgets
Cost of changing land use	6 crops, 9 years	Consultation with field experts (academia and industry)
Land	6 crops, 198 sub-basins	NLCD (2004), USDA NASS (2019)
TP loads	6 crops, 198 sub-basins, 9 years	SWAT model
Surface runoff	6 crops, 198 sub-basins, 9 years	SWAT model

Table 7

The most sensitive parameters for streamflow, total suspended solids (TSS), total phosphorus (TP), and their fitted, minimum, and maximum values used during the calibration of SWAT with SWAT-CUP.

Parameter	Description	Land use	Fitted value	Method*	Min. value	Max. value	P-value
Parameters sensitive to flow							
CH_K2.rte	Effective hydraulic conductivity of the alluvium in the main channel (mm/hr)		1.34	v	0	30	0
GW_DELAY. gw	Groundwater delay time (days)		33	v		0	0
CN2.mgt	Runoff curve number 2	Row crops Forest (HW) Forest (SW) Cotton	68 38 56 0.8 0.006	r r r v r	-0.2 -0.02 -0.02 0.15 -0.2	0.2 0.02 0.02 1 0.4	0.002 0.002 0.002 0.004 0.023
DLAI.plant	Fraction of growing season when leaf area begins to decline						
SOL_AWC.sol	Available water capacity of the soil layer (mm H ₂ O/mm soil)						
Parameters sensitive to sediment load							
SPCON.bsn	Maximum amount of sediment that can be reentrained during channel sediment routing		0.001	v	0.0001	0.01	0
SPEXP.bsn	Exponent parameter for calculating sediment reentrained in channel sediment routing		1.2	v	1	1.5	0
USLE_C.plant	Cover factor for the effect of land cover on erosion	Cotton	0.34	v	0.001	0.5	0.016
Parameters sensitive to TP load							
ERORGP.hru	Enrichment ratio for loading with sediment		2.58	v	0	5	0
RSDCO.bsn	Residue decomposition coefficient		0.07	v	0.02	0.1	0.017

* v indicates the existing parameter value is to be replaced by a given value. r means an existing parameter value is multiplied by (1 + given value).

Table 8

The simulated Kling-Gupta efficiency (KGE) and the Percent Bias (PBIAS) for TP loads (kg/ha), sediment, and streamflow during calibration and validation periods at the watershed outlet.

Simulation period	TP		Sediment		Streamflow	
	KGE	PBIAS	KGE	PBIAS	KGE	PBIAS
1997–2001 (calibration)	0.63	0.4	0.43	-2.5	0.80	2.5
2002–2003 (validation)	0.30	17.2	0.57	0.2	0.71 *	3.8 *

*For streamflow, validation simulation period was 2002–2005.

chance to meet the regulation under Scenarios 0 and 6 are \$1340/ha/yr and \$562/ha/yr, respectively. For the comparison among different probabilistic scenarios, the estimated profit using the 99 % chance constraint is consistently lower than using 90 % across the six non-baseline scenarios. The estimates with a 95 % chance constraint are somewhere between the ones for 90 % and 99 %. For instance, under Scenario 6, the profit estimates decrease from \$587/ha/yr to \$521/ha/yr when the required probability of meeting the policy standard increases from 90 % to 99 %. This outcome implies that when the model requires a higher chance to fulfill the water quality standard, the land use structure is forced to shift to crops with a lower profit but generate less pollution. More detail about the associated land use change is presented in Section 3.2.4.

Fig. 9c and Fig. 9d present the associated TP changes under Scenarios 1 and 6, respectively, given each model type. Overall, the results show that the concentration follows the water quality improvement path scenarios and natural fluctuation, as illustrated in Fig. 4 and Fig. 7, respectively. In addition, average TP (i.e., the average TP concentration over the study period) has the lowest amount under Scenario 6 and the highest amount when no policy is enforced (Scenario 0). For the comparison among the model types, TP concentration in the stochastic model is consistently equal to or higher than in deterministic ones. Numerically speaking, that is the consequence of adding a positive squared root in Eq. (10). Hence, the stochastic constraint results in a higher TP amount than the deterministic constraint, i.e., Eq. (8). The implication of this outcome indicates that considering the uncertainty of the TP concentration leads to a higher average water pollution amount (Fig. 9e). Moving from Scenario 0 to Scenario 6, the corresponding average TP concentration reduces by 39 % under SP50-DY and reduces

by 45 % under SP95-DY. In a moderate case, moving from Scenario 0 to Scenario 4, the corresponding average TP concentration decreases by 11 % and 16 % under SP50-DY and SP95-DY, respectively.

The tradeoff between TP reduction and estimated profits changes for the deterministic yield models is shown in Fig. 9f. In summary, the deterministic TP models have a higher profit and lower resulting TP concentration than the stochastic TP models. Among different policy scenarios, stricter regulation scenarios result in lower profits and TP loads than loose regulation scenarios. Among different degrees of uncertainty (i.e., SP90, SP95, SP99), the resulting TP loads are not necessarily lower as the constraint assurance level increases. That is because the objective function of the optimization model is profit maximization instead of TP load minimization. Moreover, the resulting TP loads are determined by the composition of a variety of land use rather being determined by the dominant land use type alone (more details refer to Section 3.2.4). Note that Scenarios 1, 2, and 3 have similar estimated results, so the corresponding lines and dots overlap.

3.2.3. Impact of regulation and crop yield uncertainties on profit changes

The results obtained from the simulation process are shown in Fig. 9b. The mean profit estimates under Scenario 0 and Scenario 6 estimated by the SP50-SY model are \$1268/ha/yr and \$617/ha/yr, respectively. Both estimates are lower than the result with certain crop yields (SP50-DY), which are \$1340/ha/yr and \$695/ha/yr, as presented in Fig. 9a. This indicates uncertain crop yields result in a reduction in profits. Similarly, the SP95-SY model result imposed a 95 % chance constraint on water quality, follows a similar pattern but produces overall lower profits. The mean profit results estimated by the SP95-SY under Scenario 0 and Scenario 6 are \$1268/ha/yr and \$483/ha/yr, respectively. Table 8 shows the equality tests for the means and variance of the aggregated profits between SP50-SY and SP95-SY across different scenarios. The test result suggests that the mean profits are significantly different between SP50-SY and SP95-SY across Scenarios 1–6, implying that the TP concentration and crop yield uncertainties result in lower mean profits. Nevertheless, the variance is significantly different at the 95 % confidence level only under Scenario 6.

In summary, our results show that landowners' profits are largely affected by land use, water quality improvement processes, and uncertainty of crop yields. The results suggest that providing a more extended

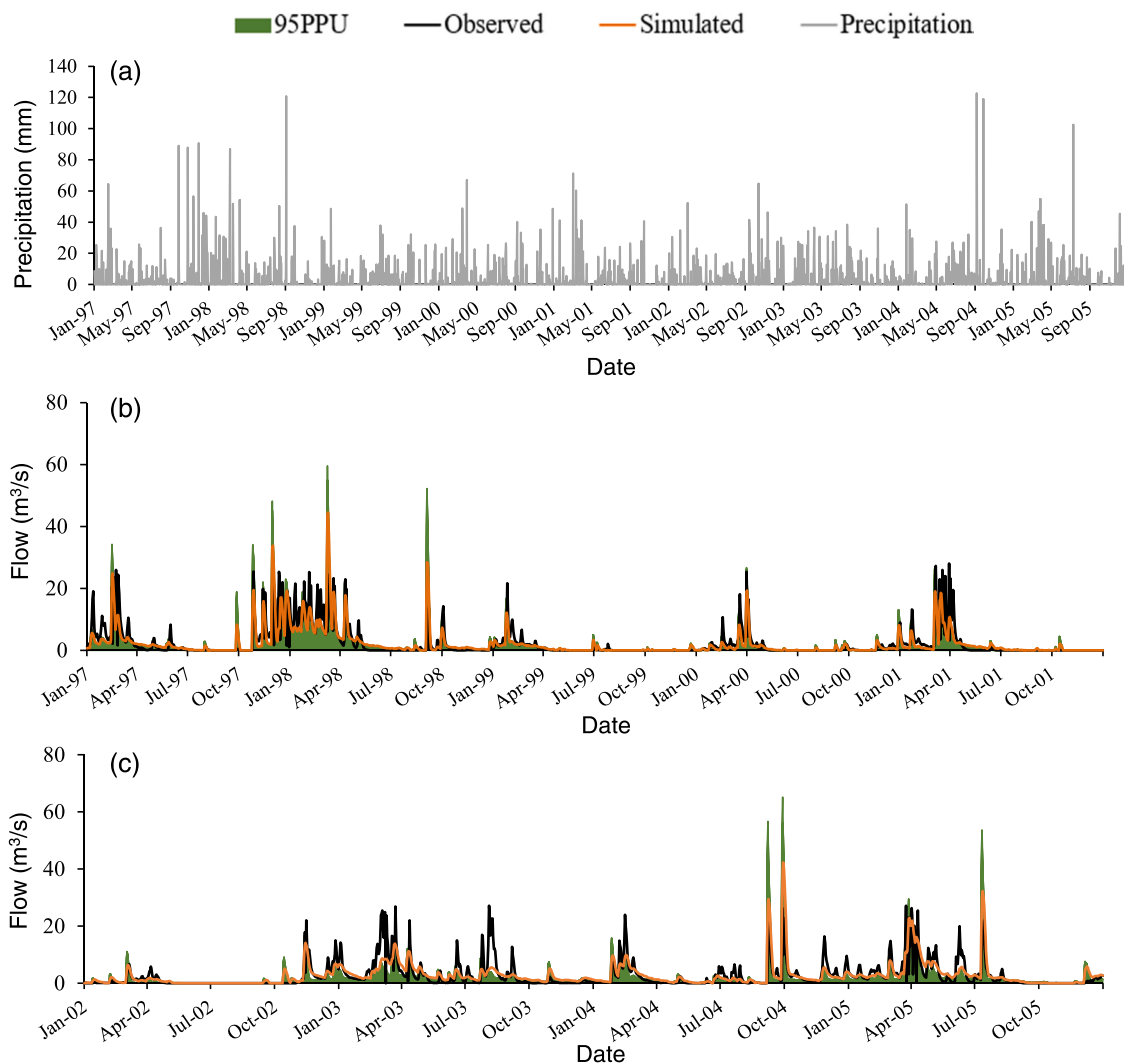


Fig. 5. Plots of daily observed precipitation, streamflow, and SWAT simulated streamflow for the best simulation, and the 95 % prediction uncertainty (95 PPU) band at the outlet of the Little River Experimental Watershed during calibration (a) and validation (b) periods.

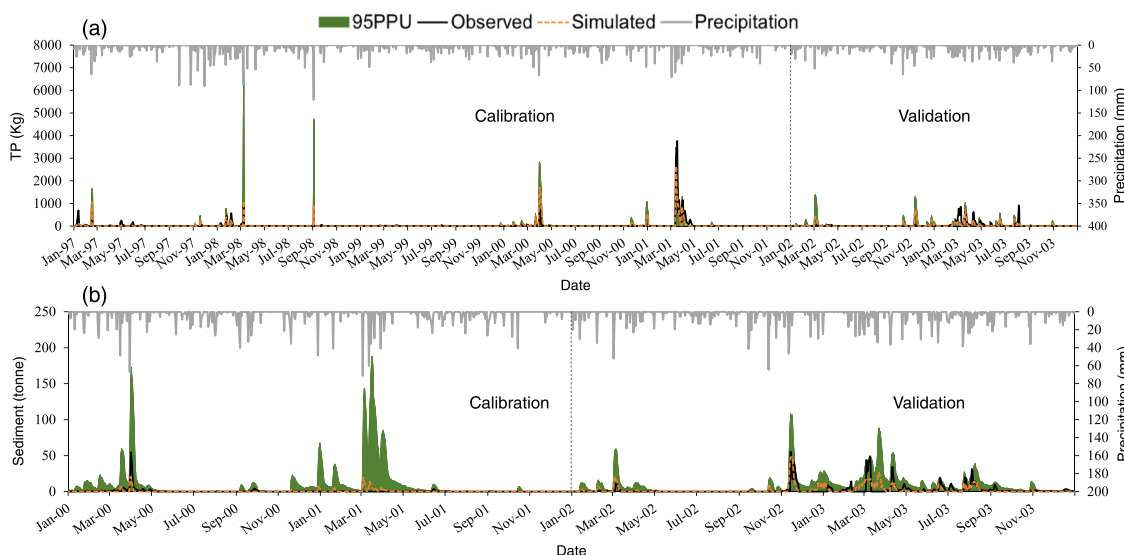


Fig. 6. Plots of daily observed, the model best fit, and 95 PPU band for TP (a) and sediment (b) loads at the outlet of Little River Experimental Watershed (LREW). 95 PPU, 95 % prediction uncertainty.

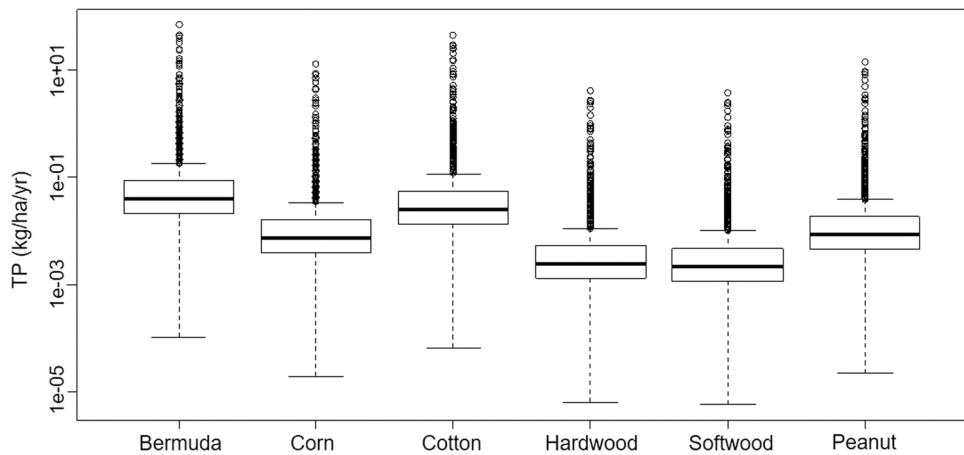


Fig. 7. Boxplots illustrating the range in TP loadings for different land classes. Points are reflective of HRU level data and depict an average of loadings over a period of nine years starting from 1997 and ending in 2005.

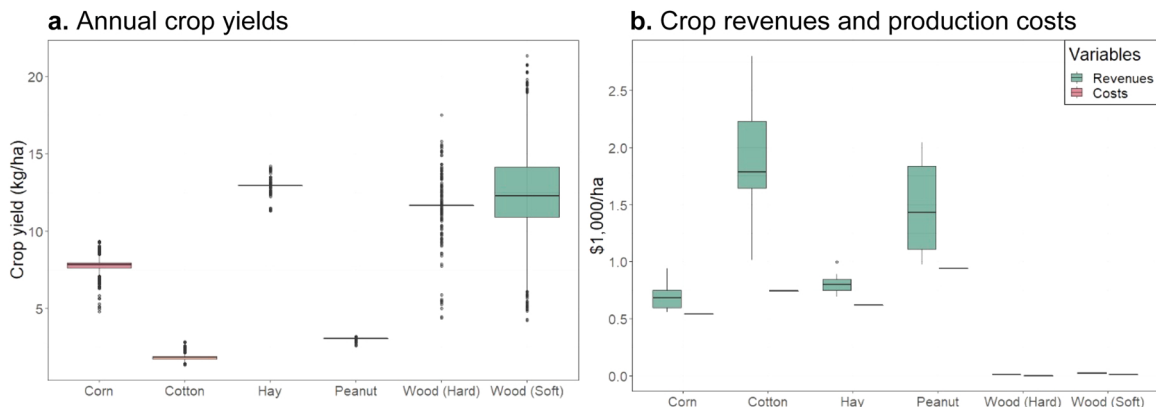


Fig. 8. Overview of economic model parameters used in the study. The demonstrated variables are crop revenues ($P_{j,i,t}$) in Panel a and crop production costs ($I_{j,t}$) in Panel b.

time period to tighten the water quality standard (e.g., Scenarios 1–3) can mitigate profit losses from rapidly switching from high-profit but high-pollutant croplands to forestlands; however, it results in higher average TP concentration. On the other hand, the adoption of more ambitious pollution mitigation (e.g., Scenario 6) leads to significantly lower aggregated profits and lower average TP concentration, namely better water quality (Table 9).

3.2.4. Impact of water pollution reduction on land use changes

To understand the underlying mechanism of the above profit changes, land use changes over the study period are investigated. Figs 10 and 11 illustrate the dominant and second dominant land use type transition in each sub-basin in both deterministic [SP50-DY] and stochastic [SP90-DY, SP95-DY, SP99-DY] dynamic optimization models under Scenario 6 from year 0 (1997) to year 8 (2005). The initial land use type is dominated by corn and softwood, and land use changes start in year 1 (1998). Deterministic model results (upper panels in Fig. 10) show that most croplands are used for planting cotton and sometimes peanut since cotton and peanut are two most profitable crops. When the water quality standard becomes stricter as time passes, the share of the hardwood land increases as hardwood has the lowest TP concentration among all crops. In some periods of time, the share of peanut replaces cotton because peanut is one of the most profitable crops but produces relatively less TP, as shown in Fig. 7.

The lower panels in Fig. 10 show the stochastic dynamic optimization model results using the chance-constraint equation (Eq. 10). The resulting optimization model allows a specific chance (e.g., 90 %, 95 %,

and 99 %) of achieving the water quality regulation standard. A comparison of the deterministic and stochastic models reveals that uncertainties of meeting the water quality standard facilitate the speed of the dominant land use type transition from croplands to forestlands and magnify the share of forestlands overall. This outcome reflects the consequence of lower profits when uncertainties of meeting the policy standard are considered.

Fig. 11 shows the transitions for the second dominant land use type under different model types. Note that sub-basins in white indicate that there is no second dominant land type. The result shows that sub-basins, which have cotton or peanut (two most profitable crops) as the dominant land use before the water quality regulation comes into effect, tend to not have the second dominant land use. This outcome likely is the consequence of maximizing profits because the profit-maximization objective leads to picking up the most profitable crop in the first place. If the model picks some less-profitable crops for some parts of sub-basins, the resulting profit won't be the maximum.

4. Discussion

Our study shows croplands can increase landowners' profit while deteriorating the water quality. This finding is aligned with previous studies investigating the relationship between water quality and agriculture in Georgia, United States. Bosch et al. (2020) analyzed 41-years of water quality data from the Little River Experimental Watershed in South Georgia reporting that chloride (Cl) concentration has increased steadily, possibly due to increased fertilization in the selected

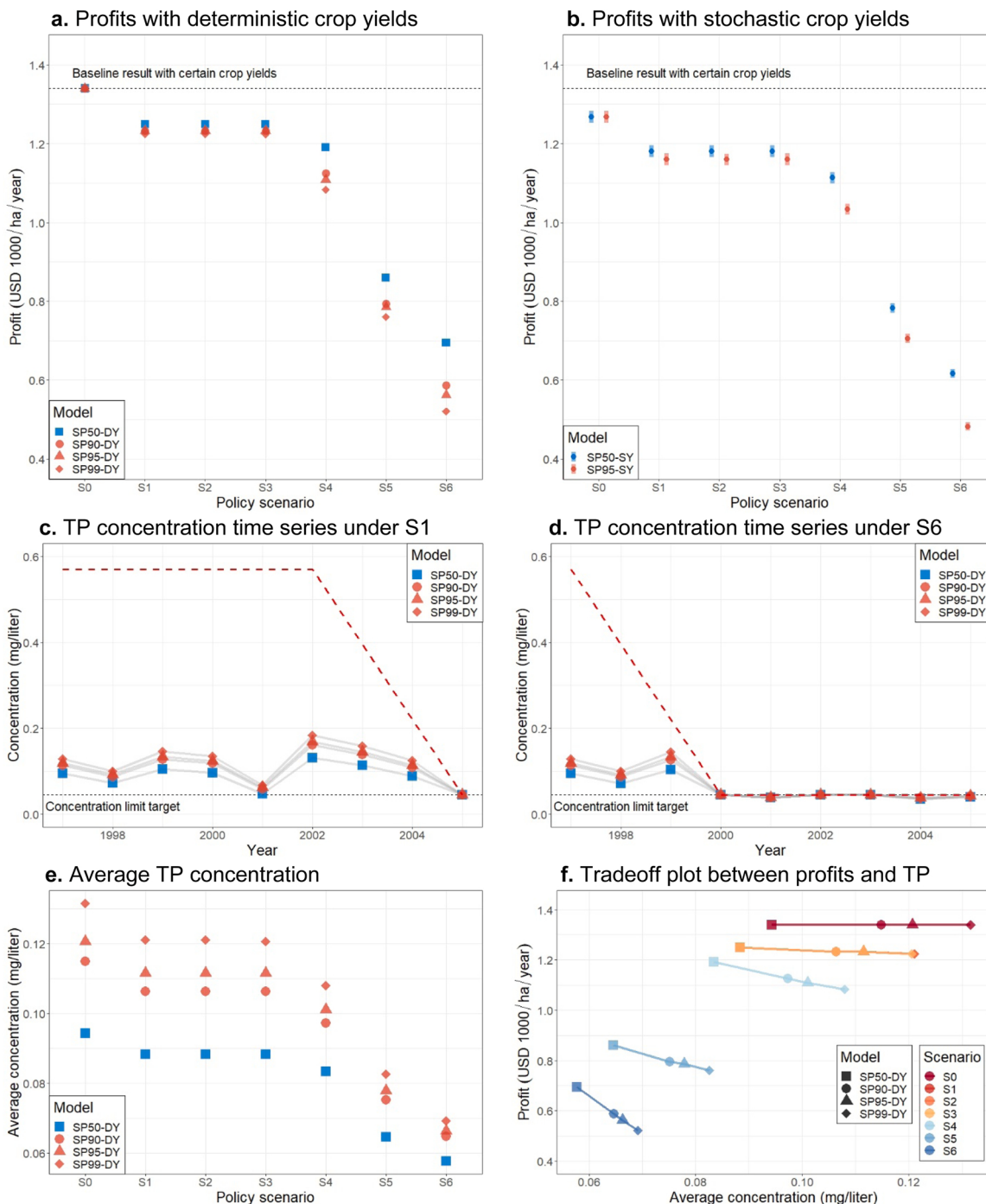


Fig. 9. Tradeoffs between TP reduction and estimated profit changes. For a comparison purpose among different model specifications under distinct policy scenarios, the horizontal dashed lines in Panels a and b indicate the profit level under the SP50-DY baseline scenario where no water quality regulation is imposed. SP90, SP95, and SP99 represent the 90 %, 95 %, and 99 % probability level of the TP concentration chance constraint, respectively. The horizontal black dashed lines in Panels c and d indicate the TP limit target (0.045 mg/L), the red dashed lines indicate the TP concentration reduction trajectory, as illustrated in Fig. 4. The average concentration of Panels e and f is the average TP concentration over the study period in each water pollution reduction scenario and model type.

Table 9

Tests for comparing means and variance of profits between SP50-SY and SP95-SY.

Scenario	S0	S1	S2	S3	S4	S5	S6
Variance	0.9770	0.4654	0.3446	0.3692	0.2721	0.1358	0.0174
Mean	0.9868	0.0000	0.0000	0.0000	0.0000	0.0000	0.0000

Note: Equality of the variances between SP50-SY and SP95-SY were tested using F-test. Equality of the means was tested using t-test if two groups have the same variance, otherwise using Wilcoxon test. The reported numbers indicate p-values from the respective test.

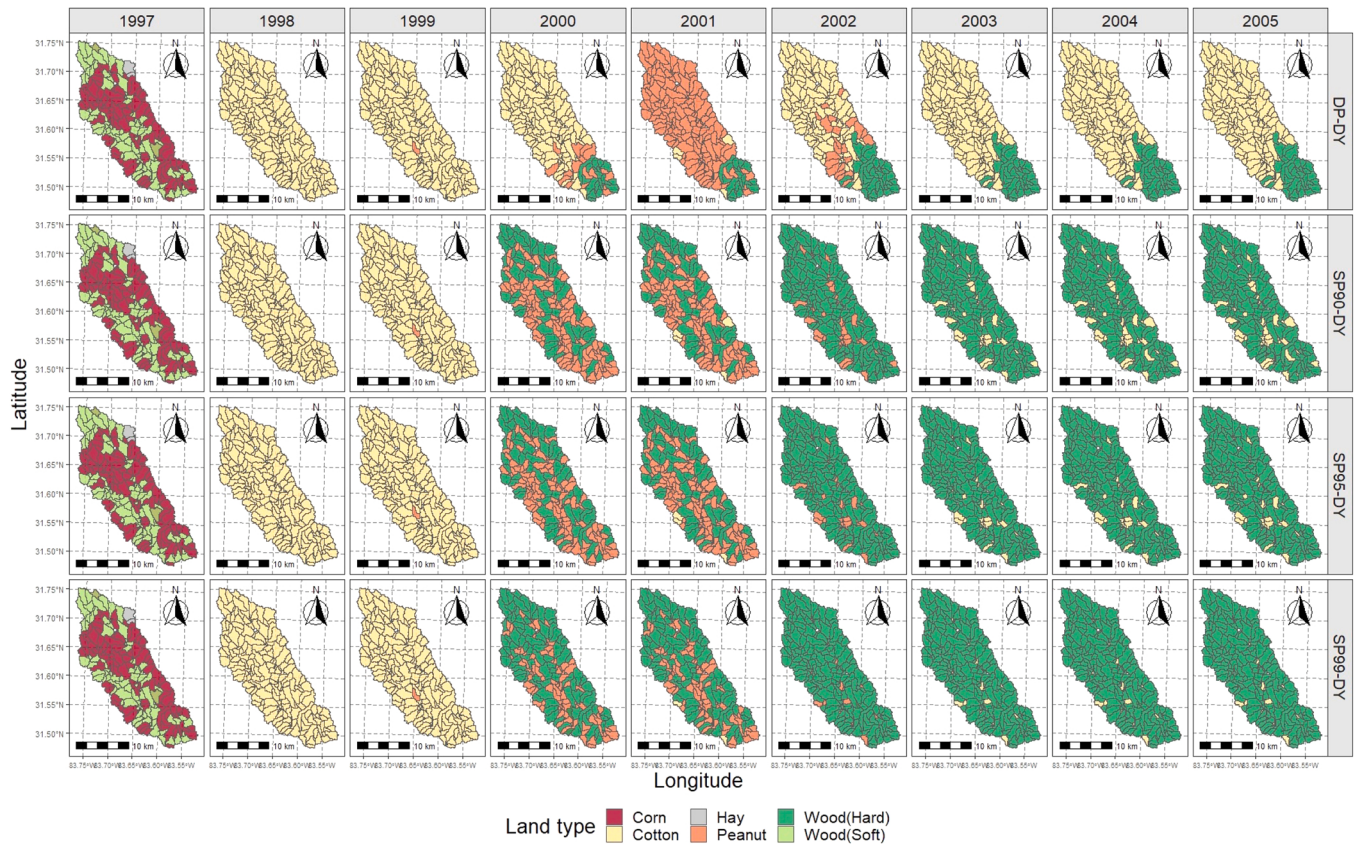


Fig. 10. Land use transitions across different model types under Scenario 6. The figures show the dominant land use type j in sub-basin i at the beginning of year t varies between different model specifications under Scenario 6.

watershed. [Bawa and Dwivedi \(2019\)](#) found that agriculture was positively associated with increased groundwater pollutants in the Suwanee River Basin. [Dalton and Frick \(2008\)](#) analyzed pesticide concentrations across 128 wells in Southwest Georgia between 1993 and 2005 and detected six compounds (atrazine, deethylatrazine, metolachlor, alachlor, fluometuron, and tebuthiuron) in more than 20 % of samples. It was also found that pesticide concentrations increased in seven wells over the selected period of the study. Similarly, other studies have also found that agriculture affects water quality in Georgia ([Duffy et al., 2020](#); [Fisher et al., 2000](#); [Yong and Chen, 2002](#)).

One of the most common practices to reduce nonpoint pollution from agriculture is to change existing croplands to forestlands. Although previous studies ([Clarke et al., 2015](#); [Rodgers et al., 2010](#)) indicate that forests may deteriorate the water quality for a short period at the stage of planting and harvesting, this study covers a relatively longer duration. It shows that forests play a crucial role in improving water quality over time. The benefit of forestlands for improving water quality is supported by several other existing studies. For example, [Tu \(2011b\)](#) analyzed 43 watersheds spread across North Georgia and found that the percentage of land under forest cover was inversely related to the level of pollutants found in the water of selected watersheds. Similar results were found in a southern Appalachian Mountain study. The relationship between levels of forest cover and water quality was investigated and showed that a higher percentage of forest cover is associated with lower suspended sediment concentrations and sediment loads ([Jackson et al., 2017](#)). Improving water quality by forests is particularly effective when forest landowners properly implement silviculture BMPs ([Cristan et al., 2016](#)). Specifically, [Griffiths et al. \(2017\)](#) investigated the effect of forestry BMPs for short-rotation pine on water quality in the Upper Coastal Plain of the Southeastern United States and showed that watersheds with intensive forestry management effectively improve water quality over time. [Rivenbark and Jackson \(2004\)](#) studied BMPs applied

in streamside management zones (SMZs) in the Georgia Piedmont and indicated that reduction of bare ground, better dispersal of road runoff, the introduction of hydraulic resistance to likely flow paths, and targeted extensions of SMZ width could prevent concentrated overland flow and associated sediment from reaching stream channels. BMPs in SMZs also are a substantial ameliorating effect on sediment transport from concentrated overland flows on clearcut sites ([Ward and Jackson, 2004](#)). The role of forestry BMPs on water quality becomes more critical as the implementation rate of forestry BMPs in Georgia has significantly risen historically and typically equals or exceeds 90 % in recent years ([Dwivedi et al., 2018](#)).

One of the issues emerging from land use changes and BMP implementation is how to create a relevant monetary incentive to encourage the adoption of BMPs and what the compensation amount for property owners would be? The results of the DWID modeling approach developed and extended in this study help us to understand the potential compensation needed for landowners to convert croplands to forestlands for improving water quality over time. Specifically, [Fig. 9](#) shows that when Scenario 0 switches to Scenario 6, the corresponding profit drops from \$1340/ha/yr to \$695/ha/yr under SP50-DY and \$562/ha/yr under SP95-DY. The associated pollution reduction is 39 % and 45 % under SP50-DY and SP95-DY, respectively. The implication of this result indicates that the resulting differences of \$645/ha/yr (\$1340/ha/yr-\$695/ha/yr) and \$778/ha/yr (\$1340/ha/yr-\$562/ha/yr) between Scenarios 0 and 6 under each model type can be viewed as proxies for willingness-to-pay of the agricultural sector to decrease TP concentrations by 39 % and 45 %. Similarly, in a moderate case, the profit reduces from \$1340/ha/yr to \$1315/ha/yr under SP50-DY and to \$1108/ha/yr under SP95-DY as Scenario 0 changes to Scenario 4. The corresponding pollution level decreases by 11 % and 16 % under SP50-DY and SP95-DY, respectively. This result indicates that the willingness-to-pay to decrease TP concentrations by 11 % and 16 % from Scenario 0 to

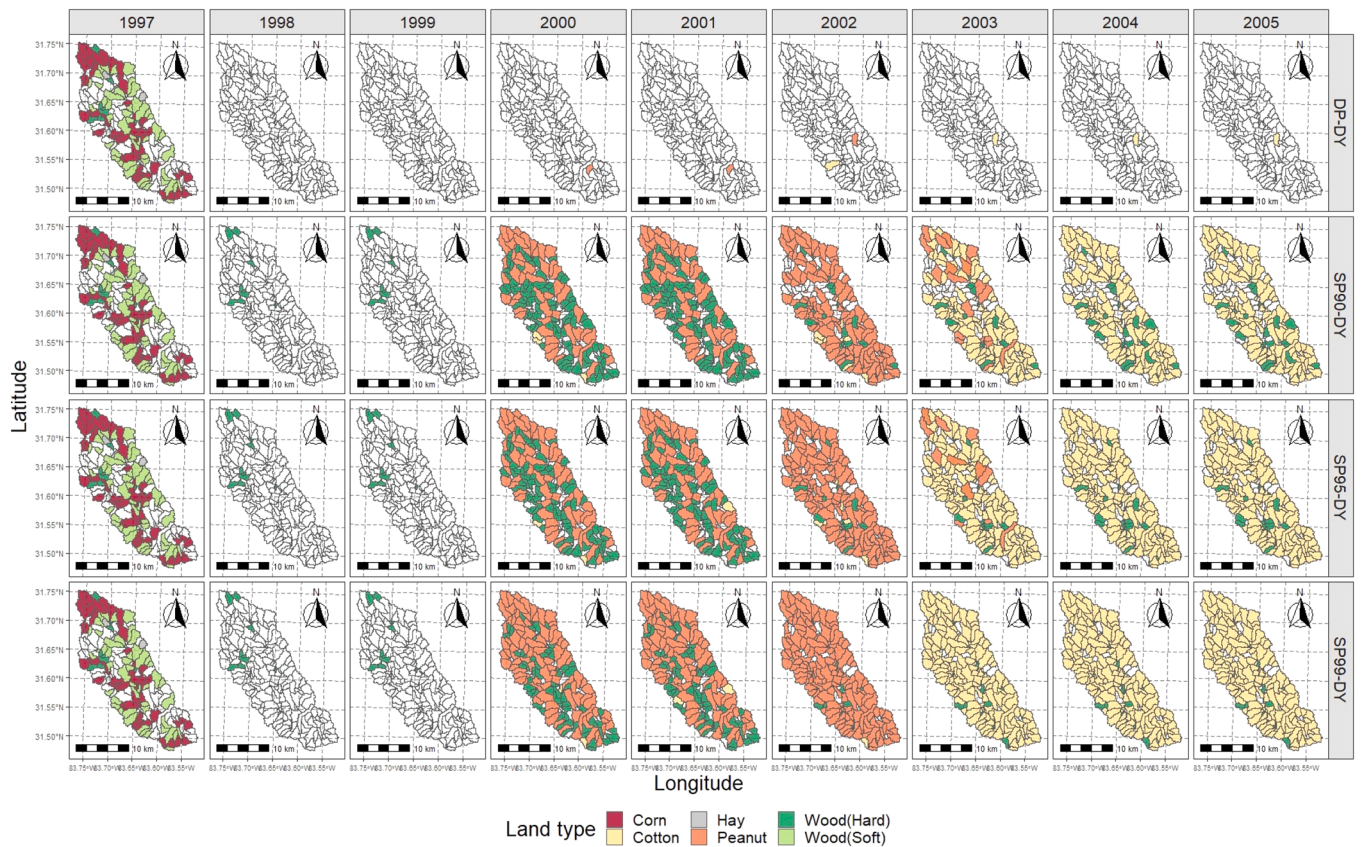


Fig. 11. Land use transitions across different model types under Scenario 6. The figures show the second dominant land use type j in sub-basin i at the beginning of year t varies between different model specifications under Scenario 6. Note: sub-basins in white indicate that there is no second dominant land type.

Scenario 4 are \$25/ha/yr and \$232/ha/yr under SP50-DY and SP95-DY, respectively. Although the Clean Water Act specifically exempts agriculture and silviculture, the above compensation payment estimates made to agricultural landowners provide relevant insights to policymakers about the cost of improving water quality by encouraging and compensating some property owners for their voluntary participation in Clean Water Act activities such as the implementation of BMPs at the watershed scale.

5. Conclusion

This study investigated the tradeoff between agricultural economic losses and potential water quality regulations at the watershed level over time. Specifically, this study applied a stochastic dynamic mathematical programming method to investigate the relationship between land use changes and water quality while considering uncertainties of meeting the water quality regulation. The result shows that, without considering the uncertainty of meeting the water quality criteria, the estimated profit is between \$1340/ha/yr and \$695/ha/yr during the study period, varying by different water quality regulation scenarios. However, when considering the uncertainty of achieving the water quality standard, the profit estimates ranged between \$1340/ha/yr and \$562/ha/yr, i.e., a reduction of 55 % relative to the deterministic baseline results. This suggests that considering the uncertainty of satisfying the water quality criteria, which is more informative, provides more conservative profit estimates. The positive relationship between losses and the degree of uncertainty is also aligned with Zhou et al. (2018), but this study provides further insights into the dynamic relationship between profits, land use changes, and water quality. The result also indicates a higher profit when providing a more extended period to tighten the water quality standard. Furthermore, the findings also show that uncertainties of meeting the water quality standard facilitate the

speed of the land use transition from croplands to forest lands and magnify the share of forestlands, highlighting the crucial role of forests in improving water quality in Georgia.

In addition, this study also examined how the profit changes while having uncertain crop yields on top of the uncertainty of meeting the water quality regulation. The result was derived from the simulation technique and showed that the estimated profit further down to \$1268/ha/yr - \$483/ha/yr (i.e., about 6–59 % lower than the SP50-DY model), varying by different policy trajectory scenarios. Similarly, profit estimates are higher under policy trajectory scenarios with a more extended adaptation period to tighten the water quality standard. Namely, the result indicates that providing a more extended period to tighten the water quality standard (Scenarios 1–3) can mitigate economic losses by rapidly switching from high-profit but high-pollutant croplands to forestlands. This suggests that once policymakers determine the water quality standard, giving landowners sufficient time to adopt the policy and adjusting land use can help landowners secure their profit while improving water quality.

Our study demonstrated that taking the uncertainty of meeting the water quality regulations and the uncertainty of crop yields into account reflects a more informative optimization setting and produces a more conservative profit estimate. Our findings suggest the importance of setting future crop yield and policy expectations for landowners. When landowners face lower yield variance (i.e., fewer uncertainties), their profit appears to be higher. Hence, providing precise crop yield forecast information based on long-term climate (e.g., El Niño, decadal climate variation) pattern prediction (Fan et al., 2017; Wang et al., 2021) or promoting crop insurance could help landowners encounter fewer uncertainties and secure their profit. Further work is needed to identify the effect of climate change on land use change. Moreover, this study assumes farmers make a decision as individually independent profit maximizers. More information on how social networks affect the

proposed land use model would help us to establish a greater degree of accuracy on related findings. This study also used default SWAT assumptions for modeling forestlands located in the study area. Further work is needed to improve the assumptions for precisely defining the role of forestlands in improving the water quality relative to actual forest practices undertaken by forest landowners in the study area. We hope that the insights developed in the study could feed into watershed-level planning and management initiatives worldwide to strike a balance between economics and environmental quality to ensure the sustainable management of watersheds.

Declaration of Competing Interest

The authors declare that they have no known competing financial interests or personal relationships that could have appeared to influence the work reported in this paper.

Data Availability

Data will be made available on request.

Acknowledgment

This research is supported by the National Institute of Food and Agriculture, United States Department of Agriculture, under award number 2017-68007-26319.

References

- Abbaspour, K.C., Rouholahnejad, E., Vaghefi, S., Srinivasan, R., Yang, H., Kløve, B., 2015. A continental-scale hydrology and water quality model for Europe: Calibration and uncertainty of a high-resolution large-scale SWAT model. *Journal of Hydrology* 524, 733–752. <https://doi.org/10.1016/J.JHYDROL.2015.03.027>.
- Abbaspour, K.C., Yang, J., Maximov, I., Siber, R., Bogner, K., Mieleitner, J., Zobrist, J., Srinivasan, R., 2007. Modelling hydrology and water quality in the pre-alpine/alpine thur watershed using SWAT. *J. Hydrol.* 333, 413–430. <https://doi.org/10.1016/J.JHYDROL.2006.09.014>.
- Arnold, J.G., Fohrer, N., 2005. SWAT2000: current capabilities and research opportunities in applied watershed modelling. *Hydrolog. Process.* 19, 563–572. <https://doi.org/10.1002/HYP.5611>.
- Arnold, J.G., Allen, P.M., Muttiah, R., Bernhardt, G., 1995. Automated base flow separation and recession analysis techniques. *Groundwater* 33, 1010–1018. <https://doi.org/10.1111/J.1745-6584.1995.TB00046.X>.
- Bawa, R., 2021. Ecological and Economic Tradeoffs associated with Land Cover Change and Water Services in southeast United States (Ph.D. Dissertation). University of Georgia, Athens, Georgia, U.S.A.
- Bawa, R., Dwivedi, P., 2019. Impact of land cover on groundwater quality in the upper floridan aquifer in Florida, United States. *Environ. Pollut.* 252, 1828–1840. <https://doi.org/10.1016/J.ENVPOL.2019.06.054>.
- Bhattarai, G., Srivastava, P., Marzen, L., Hite, D., Hatch, U., 2008. Assessment of economic and water quality impacts of land use change using a simple bioeconomic model. *Environ. Manag.* 42, 122–131. <https://doi.org/10.1007/S00267-008-9111-9>.
- Boadu, F., McCarl, B., Gillig, D., 2007. An empirical investigation of institutional change in groundwater management in Texas: the edwards aquifer case. *Nat. Resour. J.* 47, 117–163.
- Bosch, D.D., Sheridan, J.M., 2007. Stream discharge database, little river experimental watershed, Georgia, United States. *Water Resour. Res.* 43. <https://doi.org/10.1029/2006WR005833>.
- Bosch, D.D., Pisani, O., Coffin, A.W., Strickland, T.C., 2020. Water quality and land cover in the Coastal Plain Little River watershed, Georgia, United States. *J. Soil Water Conserv.* 75, 263–277. <https://doi.org/10.2489/JSWC.75.3.263>.
- Cardwell, H., Ellis, H., 1993. Stochastic dynamic programming models for water quality management. *Water Resour. Res.* 29, 803–813. <https://doi.org/10.1029/93WR00182>.
- Chen, C.-C., McCarl, B.A., Williams, R.L., 2006. Elevation dependent management of the edwards aquifer: linked mathematical and dynamic programming approach. *J. Water Resour. Plan. Manag.* 132, 330–340. [https://doi.org/10.1061/\(ASCE\)0733-9496\(2006\)132:5\(330\)](https://doi.org/10.1061/(ASCE)0733-9496(2006)132:5(330)).
- Clarke, J., Kelly-Quinn, M., Blacklocke, S., Bruen, M., 2015. The effect of forest windrowing on physico-chemical water quality in Ireland. *Sci. Total Environ.* 514, 155–169. <https://doi.org/10.1016/j.scitotenv.2015.01.107>.
- Cristan, R., Aust, W.M., Bolding, M.C., Barrett, S.M., Munsell, J.F., Schilling, E., 2016. Effectiveness of forestry best management practices in the United States: literature review. *For. Ecol. Manag.* 360, 133–151. <https://doi.org/10.1016/J.FORECO.2015.10.025>.
- Cristan, R., Michael Aust, W., Chad Bolding, M., Barrett, S.M., Munsell, J.F., 2018. National status of state developed and implemented forestry best management practices for protecting water quality in the United States. *For. Ecol. Manag.* 418, 73–84. <https://doi.org/10.1016/J.FORECO.2017.07.002>.
- Dalton, M.S., Frick, E.A., 2008. Fate and transport of pesticides in the ground water systems of Southwest Georgia, 1993–2005. *J. Environ. Qual.* 264. <https://doi.org/10.2134/JEQ2007.0163>.
- Duffy, C., O'Donoghue, C., Ryan, M., Kilcline, K., Upton, V., Spillane, C., 2020. The impact of forestry as a land use on water quality outcomes: an integrated analysis. *For. Policy Econ.* 116. <https://doi.org/10.1016/j.forepol.2020.102185>.
- Dwivedi, P., Tumpach, C., Cook, C., Izlar, B., 2018. Effects of the sustainable forestry initiative fiber sourcing standard on the average implementation rate of forestry best management practices in Georgia, United States. *For. Policy Econ.* 97, 51–58. <https://doi.org/10.1016/J.FOREPOL.2018.08.016>.
- Ellis, J.H., 1987. Stochastic water quality optimization using imbedded chance constraints. *Water Resour. Res.* 23, 2227–2238. <https://doi.org/10.1029/WR023i012p02227>.
- Environmental Protection Division, 2020. Geographic Information Systems GIS Databases and Documentation [WWW Document]. URL <https://epd.georgia.gov/geographic-information-systems-gis-databases-and-documentation> (accessed 7.13.21).
- Fan, X., Fei, C.J., McCarl, B.A., 2017. Adaptation: an agricultural challenge. *Climate* 2017 Vol. 5, 56. <https://doi.org/10.3390/CLI5030056>.
- Fisher, D.S., Steiner, J.L., Endale, D.M., Stuedemann, J.A., Schomberg, H.H., Franzluebbers, A.J., Wilkinson, S.R., 2000. The relationship of land use practices to surface water quality in the upper oconee watershed of Georgia. *For. Ecol. Manag.* 128, 39–48. [https://doi.org/10.1016/S0378-1127\(99\)00270-4](https://doi.org/10.1016/S0378-1127(99)00270-4).
- Fujiwara, O., Gnanendran, S.K., Ohgaki, S., 1986. River quality management under stochastic streamflow. *J. Environ. Eng.* 112, 185–198. [https://doi.org/10.1061/\(ASCE\)0733-9372\(1986\)112:2\(185\)](https://doi.org/10.1061/(ASCE)0733-9372(1986)112:2(185)).
- Gaddis, E.J.B., Voinov, A., Seppelt, R., Rizzo, D.M., 2014. Spatial optimization of best management practices to attain water quality targets. *Water Resour. Manag.* 28, 1485–1499. <https://doi.org/10.1007/s11269-013-0503-0>.
- Gassman, P., Reyes, M., Green, C., Arnold, J., 2007. The Soil and Water Assessment Tool: Historical Development, Applications, and Future Research Directions. *Transactions of the ASABE* 50 (4), 1211. <https://doi.org/10.13031/2013.23637>.
- Georgia Environmental Protection Division, 2020. WATER QUALITY IN GEORGIA 2018–2019 (2020 Integrated 305b/303d Report).
- Gillig, D., McCarl, B.A., Boadu, F., 2001. An economic, hydrologic, and environmental assessment of water management alternative plans for the south central Texas region. *J. Agric. Appl. Econ.* 33, 59–78.
- Griffiths, N.A., Jackson, C.R., Bitew, M.M., Fortner, A.M., Fouts, K.L., McCracken, K., Phillips, J.R., 2017. Water quality effects of short-rotation pine management for bioenergy feedstocks in the southeastern United States. *For. Ecol. Manag.* 400, 181–198. <https://doi.org/10.1016/J.FORECO.2017.06.011>.
- Gunter, J.T., Hodges, D.G., Regens, J.L., 2005. Probability models for predicting local water quality regulations in the southern United States. *For. Policy Econ.* 7, 868–876. <https://doi.org/10.1016/J.FORPOL.2004.04.004>.
- Gupta, H.V., Kling, H., Yilmaz, K.K., Martinez, G.F., 2009. Decomposition of the mean squared error and NSE performance criteria: Implications for improving hydrological modelling. *Journal of Hydrology* 377 (1–2), 80–91. <https://doi.org/10.1016/J.JHYDROL.2009.08.003>.
- Haas, H., Reaver, N.G.F., Karki, R., Kalin, L., Srivastava, P., Kaplan, D.A., Gonzalez-Benecke, C., 2022. Improving the representation of forests in hydrological models. *Sci. Total Environ.* 812, 151425. <https://doi.org/10.1016/J.SCITOTENV.2021.151425>.
- Hargreaves, G.L., Hargreaves, G.H., Riley, J.P., 1985. Agricultural benefits for Senegal river basin. *J. Irrig. Drain. Eng.* 111, 113–124. [https://doi.org/10.1061/\(ASCE\)0733-9437\(1985\)111:2\(113\)](https://doi.org/10.1061/(ASCE)0733-9437(1985)111:2(113)).
- Hubbard, R.K., 1985. Characteristics of selected upland soils of the Georgia Coastal Plain. U.S. Dept. of Agriculture, Agricultural Research Service. <https://doi.org/10.3337/JQUERY-UI.JS>.
- Isik, S., Kalin, L., Schoonover, J.E., Srivastava, P., Graeme Lockaby, B., 2013. Modeling effects of changing land use/cover on daily streamflow: an artificial neural network and curve number based hybrid approach. *J. Hydrol.* 485, 103–112. <https://doi.org/10.1016/J.JHYDROL.2012.08.032>.
- Jackson, C.R., 2012. Water quality: timber harvesting. *Encyclopedia of Environmental Management*. CRC Press, pp. 2770–2775. <https://doi.org/10.1081/E-EEM-120046680>.
- Jackson, C.R., Bahn, R.A., Webster, J.R., Rhett, C., 2017. Water quality signals from rural land use and exurbanization in a mountain landscape: what's clear and what's confounded. *J. Am. Water Resour. Assoc.* 53, 1212–1228. <https://doi.org/10.1111/1752-1688.12567>.
- Jacobs, T.L., Medina, M.A., Ho, J.T., 1997. Chance constrained model for storm-water system design and rehabilitation. *J. Water Resour. Plan. Manag.* 123, 163–168. [https://doi.org/10.1061/\(ASCE\)0733-9496\(1997\)123:3\(163\)](https://doi.org/10.1061/(ASCE)0733-9496(1997)123:3(163)).
- Kaim, A., Strauch, M., Volk, M., 2020. Using stakeholder preferences to identify optimal land use configurations. *Front. Water* 2, 63. <https://doi.org/10.3389/frwa.2020.579087>.
- Kalin, L., Hantush, M.M., 2009. An auxiliary method to reduce potential adverse impacts of projected land developments: subwatershed prioritization. *Environ. Manag.* 43, 311–325. <https://doi.org/10.1007/S00267-008-9202-7>.
- Li, Q., Pizer, W.A., 2021. Use of the consumption discount rate for public policy over the distant future. *J. Environ. Econ. Manag.* 107, 102428. <https://doi.org/10.1016/J.JEEM.2021.102428>.
- Maggard, A., Barlow, R., 2016. Costs and trends for Southern forestry practices. *For. Land.* 76, 31–39.

- Moriasi, D.N., Arnold, J.G., Liew, M.W., van, Bingner, R.L., Harmel, R.D., Veith, T.L., 2007. Model Evaluation Guidelines for Systematic Quantification of Accuracy in Watershed Simulations. *Trans. ASABE* 50, 885–900. <https://doi.org/10.13031/2013.23153>.
- Moriasi, D.N., Wilson, B.N., Douglas-Mankin, K.R., Arnold, J.G., Gowda, P.H., 2012. Hydrologic and water quality models: use, calibration, and validation. *Trans. ASABE* 55, 1241–1247. <https://doi.org/10.13031/2013.42265>.
- Moriasi, D.N., Gitau, M.W., Pai, N., Daggupati, P., 2015. Hydrologic and water quality models: performance measures and evaluation criteria. *Trans. ASABE* 58, 1763–1785. <https://doi.org/10.13031/TRANS.58.10715>.
- Neary, D.G., Ice, G.G., Jackson, C.R., 2009. Linkages between forest soils and water quality and quantity. *For. Ecol. Manag.* 258, 2269–2281. <https://doi.org/10.1016/J.FORECO.2009.05.027>.
- NLCD, 2004. U.S. Geological Survey, National Land Cover Database [WWW Document]. URL <https://www.usgs.gov/centers/eros/science/national-land-cover-database> (accessed 3.27.22).
- Noori, N., Kalin, L., Sen, S., Srivastava, P., Lebleu, C., 2016. Identifying areas sensitive to land use/land cover change for downstream flooding in a coastal Alabama watershed. *Reg. Environ. Change* 16, 1833–1845. <https://doi.org/10.1007/S10113-016-0931-5>.
- Office of Management and Budget, 1992. Circular No. A-94 – Guidelines and Discount Rates for Benefit-Cost Analysis of Federal Programs [WWW Document]. URL <https://georgewbush-whitehouse.archives.gov/omb/circulars/a094/a094.html> (accessed 7.11.21).
- Pennington, D.N., Dalzell, B., Nelson, E., Mulla, D., Taff, S., Hawthorne, P., Polasky, S., 2017. Cost-effective land use planning: optimizing land use and land management patterns to maximize social benefits. *Ecol. Econ.* 139, 75–90. <https://doi.org/10.1016/J.ECOLECON.2017.04.024>.
- Rabotyagov, S., Campbell, T., Jha, M., Gassman, P.W., Arnold, J., Kurkalova, L., Seecchi, S., Feng, H., Kling, C.L., 2010. Least-cost control of agricultural nutrient contributions to the Gulf of Mexico hypoxic zone. *Ecol. Appl.* 20, 1542–1555. <https://doi.org/10.1890/08-0680.1>.
- Reckhow, K.H., Beaulac, M.N., Simpson, J.T., 1980. Modeling phosphorus loading and lake response under uncertainty: A manual and compilation of export coefficients.
- Rivenbark, B.L., Jackson, C.R., 2004. Concentrated flow breakthroughs moving through silvicultural streamside management zones: Southeastern Piedmont, USA. *J. Am. Water Resour. Assoc.* 40, 1043–1052. <https://doi.org/10.1111/J.1752-1688.2004.TB01065.X>.
- Rodgers, M., O'Connor, M., Healy, M.G., O'Driscoll, C., Asam, Z.U.Z., Nieminen, M., Poole, R., Müller, M., Xiao, L., 2010. Phosphorus release from forest harvesting on an upland blanket peat catchment. *For. Ecol. Manag.* 260, 2241–2248. <https://doi.org/10.1016/j.foreco.2010.09.037>.
- Saghafian, B., Khosroshahi, M., 2005. Unit response approach for priority determination of flood source areas. *J. Hydrol. Eng.* 10, 270–277. [https://doi.org/10.1061/\(ASCE\)1084-0699\(2005\)10:4\(270\)](https://doi.org/10.1061/(ASCE)1084-0699(2005)10:4(270)).
- Schüerz, C., 2019. SWATplusR: running SWAT2012 and SWAT+. Proj. R. <https://doi.org/10.5281/zenodo.3373859>.
- Sethi, L.N., Panda, S.N., Nayak, M.K., 2006. Optimal crop planning and water resources allocation in a coastal groundwater basin, Orissa, India. *Agric. Water Manag.* 83, 209–220. <https://doi.org/10.1016/j.agwat.2005.11.009>.
- Singh, H.V., Kalin, L., Morrison, A., Srivastava, P., Lockaby, G., Pan, S., 2015. Post-validation of SWAT model in a coastal watershed for predicting land use/cover change impacts. *Hydrolog. Res.* 46, 837–853. <https://doi.org/10.2166/NH.2015.222>.
- Shrestha, S., Dwivedi, P., McKay, S.K., Radcliffe, D., 2019. Assessing the Potential Impact of Rising Production of Industrial Wood Pellets on Streamflow in the Presence of Projected Changes in Land Use and Climate: A Case Study from the Oconee River Basin in Georgia. *United States. Water* 11 (1), 142. <https://doi.org/10.3390/W11010142>.
- Sunandar, A.D., Suhendang, E., Jaya, N.S., 2014. Land use optimization in asahan watershed with linear programming and SWAT model plant medicine from highland forest view project land use optimization in asahan watershed with linear programming and SWAT model. *Artic. Int. J. Sci.: Basic Appl. Res.* 18, 63–78.
- TMS, 2019. TimberMart-South Quarterly Report. Norris foundation, Athens, Georgia.
- Tu, J., 2011a. Spatial variations in the relationships between land use and water quality across an urbanization gradient in the watersheds of northern Georgia, USA. *Environ. Manag.* 51, 1–17. <https://doi.org/10.1007/S00267-011-9738-9>.
- Tu, J., 2011b. Spatial and temporal relationships between water quality and land use in northern Georgia, USA. *J. Integr. Environ. Sci.* 8, 151–170. <https://doi.org/10.1080/1943815X.2011.577076>.
- University of Georgia, C. of A. & E.S.E., 2020. Extension [WWW Document]. University of Georgia, College of Agricultural & Environmental Sciences. URL <https://agecon.uga.edu/extension/budgets/historical-budgets.html> (accessed 4.27.21).
- USDA-NASS, 1997. United States Department of Agriculture, National Agricultural Statistics Service, National Crop Progress [WWW Document]. URL https://www.nass.usda.gov/Publications/National_Crop_Progress/ (accessed 2.6.22).
- USDA-NASS, 2019. United States Department of Agriculture, National Agricultural Statistics Service [WWW Document]. URL <https://data.nal.usda.gov/dataset/nassquick-stats>.
- USDA-NRCS, 2021. United States Department of Agriculture, Natural Resources Conservation Service: Geospatial Data Gateway [WWW Document]. URL <https://datagateway.ncrs.usda.gov/> (accessed 6.2.22).
- USEPA, 2014. U.S. Environmental Protection Agency, Summary Table for the Nutrient Criteria Documents. <https://www.epa.gov/sites/production/files/2014-08/documents/criteria-nutrient-ecoregions-sumtable.pdf>.
- USEPA, 2015. U.S. Environmental Protection Agency, Total Phosphorus [WWW Document]. URL <https://www.epa.gov/sites/production/files/2015-09/documents/totalphosphorus.pdf> (accessed 4.20.21).
- USEPA, 2020. U.S. Environmental Protection Agency, National Rivers and Streams Assessment 2013–2014: Federal Partners.
- USGS, 2016. U.S. Geological Survey, Groundwater Atlas of the United States (HA 730-G).
- USGS, 2022. U.S. Geological Survey, Water Resources: About USGS Water Resources [WWW Document]. URL <https://water.usgs.gov/GIS/huc.html> (accessed 3.14.22).
- van Liew, M.W., Arnold, J.G., Bosch, D.D., 2005. Problems and potential of autocalibrating a hydrologic model. *Trans. ASAE* 48, 1025–1040. <https://doi.org/10.13031/2013.18514>.
- Wang, M., Huang, Y.-K., Cheng, M., Sheng, B., McCarl, B., 2021. El Niño southern oscillation and decadal climate variability impacts on crop yields and adaptation value. *CAB Rev.: Perspect. Agric., Vet. Sci., Nutr. Nat. Resour.* 16, 1–13. <https://doi.org/10.1079/PAVSNRR202116043>.
- Wang, S., Huang, G.H., Zhou, Y., 2015. Inexact probabilistic optimization model and its application to flood diversion planning in a dynamic and uncertain environment. *J. Water Resour. Plan. Manag.* 141, 04014093, 10.1061/(ASCE)WR.1943-5452.0000492.
- Ward, J.M., Jackson, C.R., 2004. Sediment trapping within forestry streamside management zones: Georgia Piedmont, USA. *J. Am. Water Resour. Assoc.* 40, 1421–1431. <https://doi.org/10.1111/J.1752-1688.2004.TB01596.X>.
- West, B., 2002. AQUA-1: water quality in the south. *South. For. Resour. Assess.* 19.
- Whittaker, G., 2005. Application of SWAT in the evaluation of salmon habitat remediation policy. *Hydrolog. Process.: Int. J.* 19, 839–848. <https://doi.org/10.1002/hyp.5615>.
- Yong, S.T.Y., Chen, W., 2002. Modeling the relationship between land use and surface water quality. *J. Environ. Manag.* 66, 377–393. <https://doi.org/10.1006/jema.2002.0593>.
- Zhou, Y., Yang, B., Han, J., Huang, Y., 2018. Robust linear programming and its application to water and environmental decision-making under uncertainty. *Sustainability* 11, 33. <https://doi.org/10.3390/su11010033>.